



A Journal of the Gesellschaft Deutscher Chemiker

# Angewandte Chemie

GDCh

International Edition

www.angewandte.org

## Accepted Article

**Title:** Self-Boosting Catalytic Nanoreactor Integrated with Triggerable Crosslinking Membrane Networks for Initiation of Immunogenic Cell Death by Pyroptosis

**Authors:** Junjie Li, Yasutaka Anraku, and Kazunori Kataoka

This manuscript has been accepted after peer review and appears as an Accepted Article online prior to editing, proofing, and formal publication of the final Version of Record (VoR). This work is currently citable by using the Digital Object Identifier (DOI) given below. The VoR will be published online in Early View as soon as possible and may be different to this Accepted Article as a result of editing. Readers should obtain the VoR from the journal website shown below when it is published to ensure accuracy of information. The authors are responsible for the content of this Accepted Article.

**To be cited as:** *Angew. Chem. Int. Ed.* 10.1002/anie.202004180

**Link to VoR:** <https://doi.org/10.1002/anie.202004180>

# Self-Boosting Catalytic Nanoreactor Integrated with Triggerable Crosslinking Membrane Networks for Initiation of Immunogenic Cell Death by Pyroptosis

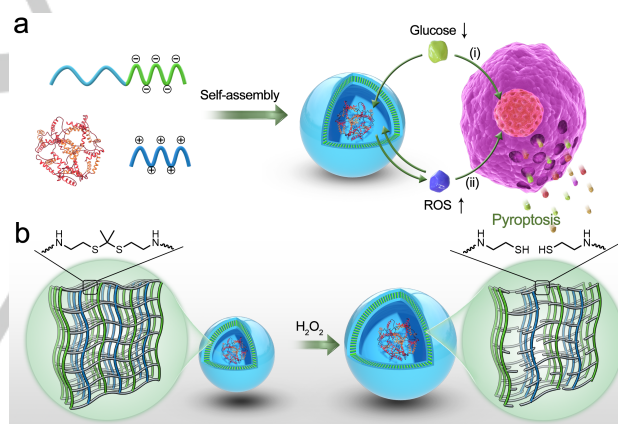
Junjie Li,\* Yasutaka Anraku, and Kazunori Kataoka\*

**Abstract:** Synthetic polymer vesicles spur novel strategies for producing biologically intelligent nanodevices with precise and specific functions (e.g. nanoreactors). Engineering vesicular nanodevices with tunable permeability by a general platform without involving trade-offs between structural integrity, flexibility and functionality remains challenging. Here, we present a general strategy to construct responsive nanoreactors based on polyion complex vesicles by integrating stimuli-responsive linkers into crosslinking membrane network. The formulated ROS-responsive nanoreactor with self-boosting catalytic glucose oxidation could protect glucose oxidase (GOD) to maintain long-term activity to achieve cytotoxic function by oxidative stress induction and glucose starvation, which is ascribed to stimuli-responsive vesicle expansion without fracture and size-selective cargo release behavior. The GOD-loaded therapeutic nanoreactor induced an immunostimulatory form of cell death by pyroptosis, which has the great potential to prime anti-tumor immune responses.

Synthetic polymer vesicles featured with hydrophilic cavity and hydrophobic membrane enable innovative nanodevices design, such as intelligent drug delivery systems, nanoswimmers, nanoreactors, and artificial organelles and cells.<sup>[1]</sup> They adapt to the surrounding environment with precise and specific functions. A key prerequisite to function precisely is to endow the vesicular membrane with tunable permeability, which should be without accompanying impaired capability as a protective layer for the encapsulated catalysts. Current strategies available for enhancing membrane permeability include incorporating stimuli-responsive polymers or channel proteins into membrane or using intrinsically permeable polymers.<sup>[2]</sup> Despite permeability enhancement in these designs, limitations remain, such as time-consuming sample processing, organic solvents contaminations, and vesicle structure damage. Furthermore, there is a barrier to extend specific designs to other responsive systems. Thus, engineering vesicular nanodevices with tunable permeability

without involving trade-offs between structural integrity, flexibility and functionality by a general platform remains challenging.

Polyion complex vesicles (PICsomes), based on electrostatic self-assembly of charge-matched polypeptides, have been developed as nanoreactor toward nanomedicine application.<sup>[2b, 3]</sup> The covalent crosslinking of PICsomes membrane creates hyperstable structure, while it simultaneously compromises membrane permeability. Interestingly, the crosslinking density would be a paramount parameter for membrane permeability.<sup>3d</sup> However, permeability regulation through the density of permanent crosslinking does not allow for achieving precise and specific functions. A rationalized strategy for designing smart nanoreactor is to integrate stimuli-responsive linkers into crosslinking membrane network.<sup>[2e, 2g, 4]</sup>



**Scheme 1.** (a) Schematic illustration of the ROS-responsive GOD-loaded therapeutic nanoreactor with self-boosting catalytic glucose oxidation due to membrane permeability enhancement during ROS production for achieving cytotoxic function via pyroptosis-mediated immunogenic cell death followed by glucose starvation (i) and oxidative stress induction (ii). (b) Schematic illustration of vesicle swelling from membranal crosslinking density decreasing and membranal hydrophobic-to-hydrophilic transition followed by  $\text{H}_2\text{O}_2$ -triggered cleavage of hydrophobic thioether linker into hydrophilic thiols.

[\*] Dr. J. Li, Prof. Dr. K. Kataoka  
Innovation Center of NanoMedicine, Kawasaki Institute of Industrial Promotion, 3-25-14 Tonomachi, Kawasaki-ku, Kawasaki 210-0821, Japan  
Email: li-j@kawasaki-net.ne.jp, k-kataoka@kawasaki-net.ne.jp  
Dr. Y. Anraku  
Graduate School of Engineering, The University of Tokyo  
7-3-1 Hongo, Bunkyo-ku, Tokyo 113-8656, Japan  
Prof. Dr. K. Kataoka  
Institute for Future Initiatives, The University of Tokyo, 7-3-1 Hongo, Bunkyo-ku, Tokyo 113-0033, Japan  
E-mail: kataoka@ifi.u-tokyo.ac.jp  
Supporting information for this article is given via a link at the end of the document.

Toward this concept, we arrived at glucose oxidase (GOD)-loaded reactive oxygen species (ROS)-responsive PICsomes composed of poly([2-[[1-[(2-aminoethyl)thio]-1-methylethyl]thio]ethyl]- $\alpha,\beta$ -aspartamide) (PATK) as polycation segments and PEG-*b*-poly( $\alpha,\beta$ -aspartic acid) (PEG-*b*-PAsp) as polyanion segments to validate the functionalities of the nanoreactor (Scheme 1). Upon  $\text{H}_2\text{O}_2$  exposure, gradual cleavage of ROS-responsive linker occurred, and the vesicle architecture evolved with stable swelling. Correspondingly, membrane permeability increased remarkably due to membranal

crosslinking density decreasing, membranal hydrophobic-to-hydrophilic transition, and vesicle swelling. The efficiency of catalytic glucose oxidation was anticipated to become high followed by permeability enhancement. Importantly, vesicular structure could maintain integrity without fracture during transformation, which protected the catalyst GOD from harsh environment for long-term activity. Meanwhile, GOD loaded therapeutic nanoreactor could induce immunogenic cell death by pyroptosis. To the best of our knowledge, this is the first example of self-boosting catalytic nanoreactor with the capability to initiate immunogenic cell death by pyroptosis.

Initially, ROS-responsive polycation, PATK, was designed with a ROS-cleavable linker (thioacetal) in the side chain. Quantitative aminolysis of poly( $\beta$ -benzyl-L-aspartate) (PBLA) by acetone-[bis-(2-amino-ethyl)-dithioacetal] to form PATK was confirmed by  $^1\text{H}$  NMR (Figure S1-S3). On the other hand, PEG-*b*-PBLA was transformed into polyanion, PEG-*b*-PAsp, by hydrolysis of BLA units under alkaline conditions (Figure S2-S3). The gel permeation chromatography (GPC) characterizations of PBLA, PEG-*b*-PBLA, PATK and PEG-*b*-PAsp confirmed the narrow MW distribution (Figure S4-S5). The ROS-cleavage of hydrophobic thioacetal linker into hydrophilic thiols was evaluated for PATK incubated with  $\text{H}_2\text{O}_2$  by  $^1\text{H}$  NMR (Figure S6).<sup>[5]</sup> The degradation rate agreed well with  $\text{H}_2\text{O}_2$  concentration as evidenced by comparing the integrals of thioacetal peak and the signal of by-product acetone arose from cleavage reaction. In this research,  $\text{H}_2\text{O}_2$  was chosen as a kind of ROS to investigate the related stimuli-responsive behavior.

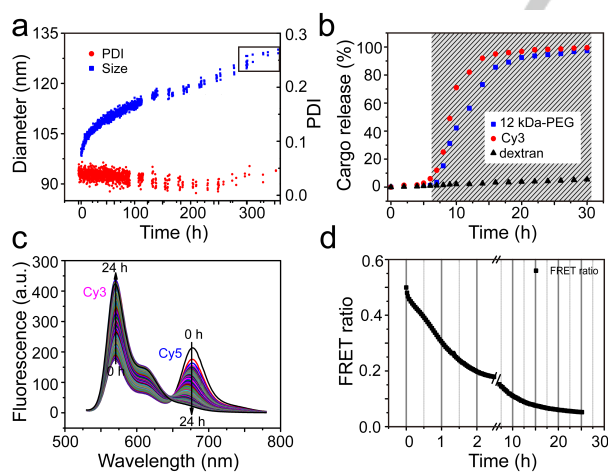


**Figure 1.** Vesicle expansion and membrane permeability enhancement of ROS-responsive PICsomes (5 mg/mL) incubated with 5 equivalents of  $\text{H}_2\text{O}_2$  to the thioacetal linker. (a) Time-dependent DLS analysis of size and size distribution (PDI) of PICsomes incubated with  $\text{H}_2\text{O}_2$ . After 300 hours, size showed little change as indicated by black rectangle. (b) Quantification of 150 kDa dextran, 12 kDa PEG, and free sulfo-Cy3 release as a function of time. Diagonal pattern indicates the addition of  $\text{H}_2\text{O}_2$ . (c) Time-dependent FRET spectra of Cy3- and Cy5-labeled PICsomes incubated with  $\text{H}_2\text{O}_2$  and (d) quantification of corresponding FRET ratio.

Using electrostatic complexation as the driving force, self-assembly of the charged polymers into PICsomes was readily performed *via* physically mixing of PATK and PEG-*b*-PAsp solutions without using organic solvents, followed by vortex for 2 min. After covalent cross-linking by 1-ethyl-3-(3-dimethylaminopropyl) carbodiimide (EDC), the stability could be further improved. TEM characterization showed the spherical vesicle structure and dynamic laser light scattering (DLS) results revealed that narrow size distribution with a polydispersity index (PDI) below 0.05 (Figure S7 and Figure 1a). To investigate the architecture transformation, 5, 50, and 100 equivalents of  $\text{H}_2\text{O}_2$  to the thioacetal linker was added into PICsomes solutions. Time-dependent DLS analysis revealed that before  $\text{H}_2\text{O}_2$  addition, the PICsomes exhibits an average diameter of about 95 nm. Upon exposure to  $\text{H}_2\text{O}_2$ , the size increased steadily without loss of narrow size distribution and culminated in a large plateau rather than fast dissociation (Figure 1a). The intact vesicular structure was verified by TEM observation (Figure S7). The long-term capability to resist fragmentation should be ascribed to incomplete breakdown of crosslinking membrane network,<sup>[6]</sup> which is often utilized as a general strategy to construct stimuli-responsive hydrogels for sustained drug release control.<sup>[7]</sup> It should be noted that the size limitation of PICsomes swelling is approximately 130 nm irrespective of  $\text{H}_2\text{O}_2$  concentration (Figure 1a and Figure S8). Along with change in dimensions, PICsomes can expand to 256 percent of original volume and 187 percent of original surface area. The increased surface area would result in loose arrangement of polymer chains, which should enhance membrane permeability. Förster resonance energy transfer (FRET) provided further insights into arrangement of polymer chains during PICsomes transformation (Figure 1c and 1d). In consistency with DLS results, FRET ratio declined significantly, especially in the initial stage of Cy3- and Cy5-labeled PICsomes transformation, indicating a loose membrane structure formation. Then, PICsomes were explored to load hydrophilic cargoes, which were simply added into solution in the process of mixing of PATK and PEG-*b*-PAsp. Size-dependent release behavior was observed (Figure 1b). For 150 kDa dextran,  $\text{H}_2\text{O}_2$ -triggered vesicle expansion had no apparent effect on the release rate. For 12 kDa PEG and free Cy3 dye,  $\text{H}_2\text{O}_2$  accelerated the release remarkably. Specifically, less than 10% of free Cy3 was released within 6 hours, but more than 80% could be released upon  $\text{H}_2\text{O}_2$  stimulation for 6 hours. Besides the loose structure from vesicle swelling, membranal crosslinking density decreasing and membranal hydrophobic-to-hydrophilic transition also account for accelerated release. The vesicle expansion without fracture and size-selective cargo release behaviors would lay a robust foundation for exploring and developing PICsomes as therapeutic nanoreactor to encapsulate some catalysts (e.g. enzyme) for running in the long-term.

Researches focus on GOD-loaded nanocarriers for cancer treatment are quickly emerging.<sup>[8]</sup> Next, GOD-loaded PICsomes (GOD@PICsomes) with 2.51% loading capacity were utilized to validate the functionalities of the formulated therapeutic nanoreactor. GOD encapsulation into PICsomes did not affect

the vesicular structure and size (Figure S9). From fluorescence correlation spectroscopy (FCS) analysis, the increased diffusion time of Cy5-labeled GOD (Cy5-GOD) loaded PICsomes compared with free Cy5-GOD implied the successful encapsulation into PICsomes (Figure S10). Glucose, a common substrate of GOD, could be catalyzed to produce  $\text{H}_2\text{O}_2$  in the presence of oxygen. It should be noted that PICsomes already had a certain degree of membrane permeability to small molecule demonstrated in our previous research,<sup>[3c]</sup> allowing glucose to slowly cross membrane. To evaluate the transformation behavior, the nanoreactor was incubated with glucose followed by size and FRET measurement. At 24 hours post incubation, Cryo-TEM characterization showed that  $\text{H}_2\text{O}_2$  from catalytic glucose oxidation triggered the nanoreactor expansion with diameter increasing from  $78 \pm 9$  nm to  $87 \pm 10$  nm, while had little effect on membranes thickness ( $17.5 \pm 1.6$  nm versus  $18.6 \pm 1.3$  nm) (Figure 2a). Even after 1-week incubation, the nanoreactor still maintained integrity with little GOD release ( $< 5\%$ ) (Figure S11).

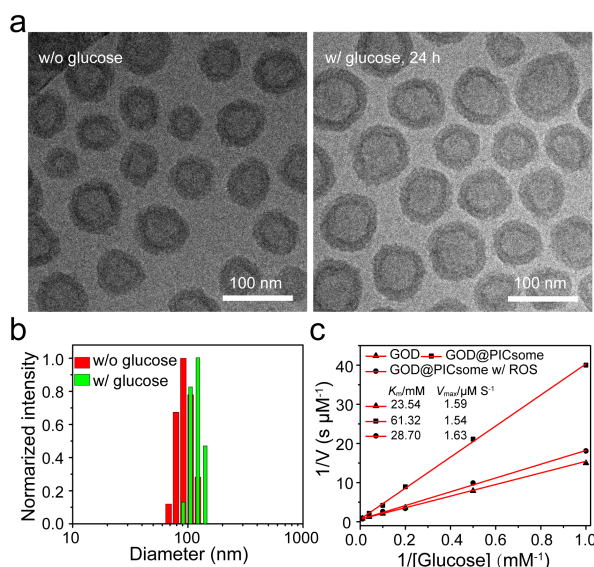


**Figure 2.** The formation and enzyme kinetic analysis of nanoreactor. (a) Cryo-TEM images and (b) DLS analysis of vesicular nanoreactor before and after treatment with 4.5 mg/mL glucose for 24 hours. (c) Kinetic parameters ( $K_m$  and  $V_{max}$ ) for GOD, GOD@PICsomes, and GOD@PICsomes pretreated with 5 equivalents of  $\text{H}_2\text{O}_2$  to the thioetal linker for 24 hours (GOD@PICsomes w/ ROS).

It is worth mentioning that the thicker membrane could be observed compared with that of previously synthesized 100-nm PICsomes,<sup>[3b]</sup> which is beneficial to high-efficacy protection and precise activation of catalysts. The nanoreactor expansion was also evidenced by DLS and FRET measurements (Figure 2b and Figure S12). The  $\text{H}_2\text{O}_2$ -triggered membrane permeability enhancement would further increase the catalytic efficiency, which endowed the nanoreactor with self-boosting capability to

amplify oxidative stress. Enzyme kinetic analysis with a Michaelis–Menten model confirmed this (Figure 2c). The catalytic efficiency of GOD decreased after encapsulating into PICsomes based on a rising Michaelis constant ( $K_m$ ) from 23.54 mM to 61.32 mM, indicating that the affinity of the substrate for GOD appears to decrease, possibly owing to the barrier effect of membrane. But pretreating nanoreactor with  $\text{H}_2\text{O}_2$  could recover the affinity apparently (28.7 mM in  $K_m$ ).<sup>[2h, 2i]</sup>

Furthermore, cytotoxic function of nanoreactor was investigated against 4T1 mouse breast cancer cells. A non-responsive nanoreactor was constructed by encapsulating GOD into previously synthesized PICsomes with similar loading capacity (2.63%) (Figures S13),<sup>[3c]</sup> which was used as a control group. IC<sub>50</sub> value of the nanoreactor was 0.15  $\mu\text{g}/\text{mL}$  compared with 0.28  $\mu\text{g}/\text{mL}$  for non-responsive nanoreactor, indicating higher cytotoxicity (Figures 3a). A plausible reason is that membrane permeability enhancement from ROS stimulation during treatment further self-boosted the capability to produce ROS for cytotoxic activity (Figure 3b). Although the toxicity of nanoreactor was lower than that of free GOD with IC<sub>50</sub> value of 0.06  $\mu\text{g}/\text{mL}$ , the nanoreactor could protect GOD to maintain long-term cytotoxic activity. We incubated 4T1 cells with free GOD and nanoreactor at their IC<sub>50</sub> concentrations, respectively. After treatment, the culture medium was collected and concentrated, followed by another treatment. The results revealed that recycled nanoreactor maintained the cytotoxic activity efficiently even after 3 cycles while free GOD lost activity quickly. A reasonable explanation is that GOD proteolysis from proteinase released from dead cells would deactivate GOD. Consistent with the cytotoxicity experiments, free GOD lost 60% activity after incubation with proteinase K for 4 hours as detected by glucose oxidase activity assay, while GOD loaded into nanoreactor kept more than 95% activity.<sup>[9]</sup>

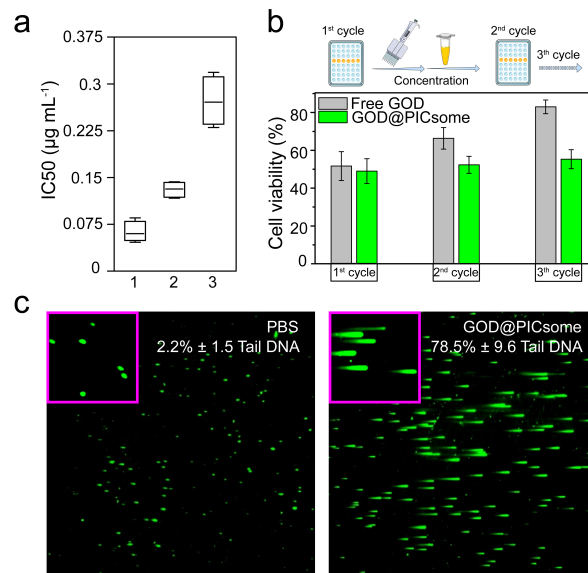


**Figure 3.** Cytocidal function of nanoreactor against 4T1 cells. (a) IC<sub>50</sub> values of GOD (1), GOD@PICsomes (2), and GOD-loaded nonresponsive nanoreactor (3). (b) Cytotoxicity of recycled GOD and GOD@PICsomes from old culture medium at their IC<sub>50</sub> concentration. (c) DNA damage of 4T1 cell treated with GOD@PICsomes at GOD concentration of 0.2  $\mu\text{g}/\text{mL}$ .

To understand the mechanism of cytotoxic action, we first evaluated the oxidative damage to cellular components (Figure S14). 78% tail DNA appeared for nanoreactor-treated cells compared with that of 2% for PBS as detected by Comet Assay, indicating severe oxidative DNA damage (Figure 3c). Real-time observation of cell morphology by confocal laser scanning microscopy (CLSM) was also conducted. After treatment with nanoreactor, the cells displayed distinctive morphology characterized with large bubbles blowing from the plasma membrane, which is a form of programmed cell death termed pyroptosis distinguished from apoptosis (Figure 4a and Figure S15).<sup>[10]</sup> The characteristic morphology could also be observed in another two cell lines, MDA-MB-231 human breast cancer cells and HT1080 human fibrosarcoma cells (Figure S16).

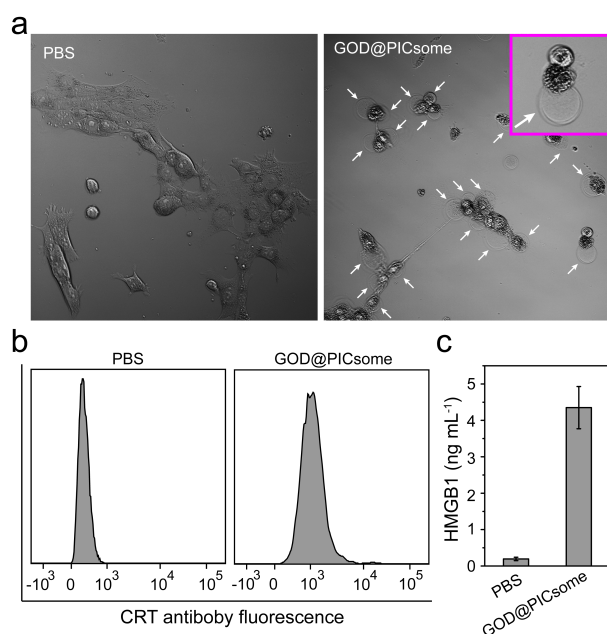


**Figure 4.** Nanoreactor-mediated immunostimulatory form of cell death by pyroptosis at GOD concentration of 0.2  $\mu\text{g}/\text{mL}$ . (a) Bright field images of 4T1 cells at 12 hours post-incubation with GOD@PICsomes. The white arrows indicated the pyroptotic cell death characterized with large bubbles blowing from the plasma membrane. (b, c) The level of immune simulants, calreticulin (b) and HMGB1 (c), for 4T1 cells at 12 hours post incubation with GOD@PICsomes.

Plasma membrane pore formation from pyroptosis causes the release of intracellular contents, including lactate dehydrogenase (LDH), pro-inflammatory cytokines (e.g. IL-1 $\beta$  and IL-18), and some immune simulants (e.g. HMGB1). More

than 85% LDH release using cell lysis as a positive control and 70% PI/Annexin V double positive cells verified the membrane pore formation (Figure S17). Level of pro-inflammatory cytokine IL-1 $\beta$  was increased in culture medium up to 20-fold (Figure S18). We further analyzed the release and cell-surface expression of immune stimulants, specifically HMGB1 and calreticulin. Nanoreactor treatment increased calreticulin expression more than 4-fold from flow cytometry analysis (Figure 4b). HMGB1 concentration also increased to 4.3 ng/mL compared with that of 0.1-0.2 ng/mL for PBS group based on ELISA assay (Figure 4c). These pro-inflammatory cytokines and immune stimulants from immunogenic cell death by pyroptosis could potentiate antitumor immune responses, as just recently highlighted in several studies.<sup>[11]</sup>

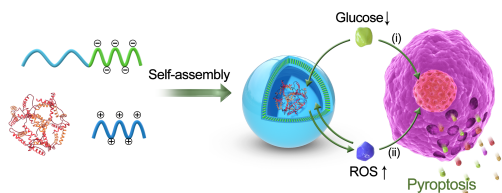
Taken together, this work provided a general platform to engineer vesicular nanodevices with tunable permeability without involving trade-offs between structural integrity, flexibility and functionality by integrating stimuli-responsive linkers into crosslinking membrane network. Given that varying polycations have already been used to form PICsomes,<sup>[3]</sup> it is feasible to extend application of this flexible strategy to other responsive vesicles. We can tailor the responsive properties in on-demand manner, for example, smart tumor microenvironment-responsive nanoreactors design. Successful fabrication of reduction-responsive PICsomes and its triggered expansion without fracture affirmed this strategy (Figure S19). Based on high oxidative stress environment and high glucose uptake in tumor site, it is reasonable to design ROS-responsive GOD-loaded nanoreactor for site-specific activation and amplification of oxidative stress, avoiding the production of excessive ROS in blood and normal tissue. However, mounting evidence indicates that “one size fits all” microenvironment does not exist in tumor. There is clearly an urgent need to construct a series of responsive vesicles with similar physicochemical properties for screening optimal nanoreactor. Furthermore, we found that GOD-loaded PICsomes as therapeutic nanoreactor with self-boosting catalytic ROS production capability and long-term cytotoxic function could induce an immunostimulatory form of cell death termed as pyroptosis, which has the great potential for priming anti-tumor immunotherapy and opens new avenues for using GOD-loaded nanocarriers as a cancer treatment modality.

## Acknowledgements

The financial support based on Center of Innovation Program (COI stream) (Project No. JPMJCE1305) from Japan Science and Technology Agency (JST) is gratefully acknowledged. J.L. thanks the financial support from JSPS International Research Fellowship (ID: P17356; Prof. Kataoka as the host researcher) and Ministry of Education, Culture, Sports, Science and Technology, Japan (MEXT) (Project No. 20K20209).

**Keywords:** Self-assembly • vesicles • nanoreactors • pyroptosis • immunogenic cell death • immunotherapy

- [1] a) P. Tanner, P. Baumann, R. Enea, O. Onaca, C. Palivan, W. Meier, *Acc. Chem. Res.* **2011**, *44*, 1039-1049; b) V. Balasubramanian, B. Herranz-Blanco, P. V. Almeida, J. Hirvonen, H. A. Santos, *Prog. Polym. Sci.* **2016**, *60*, 51-85; c) J. Gaitzsch, X. Huang, B. Voit, *Chem. Rev.* **2016**, *116*, 1053-1093; d) J. F. Mukerabigwi, Z. Ge, K. Kataoka, *Chem. Eur. J.* **2018**, *24*, 15706-15724; e) T. Patino, X. Arque, R. Mestre, L. Palacios, S. Sanchez, *Acc. Chem. Res.* **2018**, *51*, 2662-2671; f) S. Pottanam Chali, B. J. Ravoo, *Angew. Chem. Int. Ed.* **2020**, *59*, 2962-2972.
- [2] a) P. Broz, S. Driamov, J. Ziegler, N. Ben-Haim, S. Marsch, W. Meier, P. Hunziker, *Nano Lett.* **2006**, *6*, 2349-2353; b) A. Koide, A. Kishimura, K. Osada, W.-D. Jang, Y. Yamasaki, K. Kataoka, *J. Am. Chem. Soc.* **2006**, *128*, 5988-5989; c) D. M. Vriezema, P. M. Garcia, N. Sancho Oltra, N. S. Hatzakis, S. M. Kuiper, R. J. Nolte, A. E. Rowan, J. C. van Hest, *Angew. Chem. Int. Ed.* **2007**, *46*, 7378-7382; d) H. C. Chiu, Y. W. Lin, Y. F. Huang, C. K. Chuang, C. S. Chern, *Angew. Chem. Int. Ed.* **2008**, *47*, 1875-1878; e) J. Gaitzsch, D. Appelhans, L. Wang, G. Battaglia, B. Voit, *Angew. Chem. Int. Ed.* **2012**, *51*, 4448-4451; f) Q. Yan, J. Wang, Y. Yin, J. Yuan, *Angew. Chem. Int. Ed.* **2013**, *52*, 5070-5073; g) X. Wang, G. Liu, J. Hu, G. Zhang, S. Liu, *Angew. Chem. Int. Ed.* **2014**, *53*, 3138-3142; h) J. Li, A. Dirisala, Z. Ge, Y. Wang, W. Yin, W. Ke, K. Toh, J. Xie, Y. Matsumoto, Y. Anraku, K. Osada, K. Kataoka, *Angew. Chem. Int. Ed.* **2017**, *56*, 14025-14030; i) J. Li, Y. Li, Y. Wang, W. Ke, W. Chen, W. Wang, Z. Ge, *Nano Lett.* **2017**, *17*, 6983-6990; j) T. Nishimura, Y. Sasaki, K. Akiyoshi, *Adv Mater* **2017**, *29*, 1702406; k) H. Che, S. Cao, J. C. M. van Hest, *J. Am. Chem. Soc.* **2018**, *140*, 5356-5359; l) W. Ke, J. Li, F. Mohammed, Y. Wang, K. Tou, X. Liu, P. Wen, H. Kinoh, Y. Anraku, H. Chen, K. Kataoka, Z. Ge, *Acs Nano* **2019**, *13*, 2357-2369; m) T. Nishimura, S. Hirose, Y. Sasaki, K. Akiyoshi, *J. Am. Chem. Soc.* **2020**, *142*, 154-161.
- [3] a) A. Kishimura, A. Koide, K. Osada, Y. Yamasaki, K. Kataoka, *Angew. Chem. Int. Ed.* **2007**, *46*, 6085-6088; b) Y. Anraku, A. Kishimura, M. Oba, Y. Yamasaki, K. Kataoka, *J. Am. Chem. Soc.* **2010**, *132*, 1631-1636; c) Y. Anraku, A. Kishimura, M. Kamiya, S. Tanaka, T. Nomoto, K. Toh, Y. Matsumoto, S. Fukushima, D. Sueyoshi, M. R. Kano, Y. Urano, N. Nishiyama, K. Kataoka, *Angew. Chem. Int. Ed.* **2016**, *55*, 560-565; d) O. F. Mutaf, Y. Anraku, A. Kishimura, K. Kataoka, *Polymer* **2017**, *133*, 1-7.
- [4] B. M. Discher, H. Bermudez, D. A. Hammer, D. E. Discher, *J. Phys. Chem. B* **2002**, *106*, 2848-2854.
- [5] D. S. Wilson, G. Dalmaso, L. Wang, S. V. Sitaraman, D. Merlin, N. Murthy, *Nat. Mater.* **2010**, *9*, 923-928.
- [6] a) A. Napoli, M. Valentini, N. Tirelli, M. Muller, J. A. Hubbell, *Nat. Mater.* **2004**, *3*, 183-189; b) A. Napoli, M. J. Boerakker, N. Tirelli, R. J. M. Nolte, N. A. J. M. Sommerdijk, J. A. Hubbell, *Langmuir* **2004**, *20*, 3487-3491.
- [7] J. Li, D. J. Mooney, *Nat. Rev. Mater.* **2016**, *1*, 16071.
- [8] L. H. Fu, C. Qi, J. Lin, P. Huang, *Chem. Soc. Rev.* **2018**, *47*, 6454-6472.
- [9] S.-M. Jo, F. R. Wurm, K. Landfester, *Nano Lett.* **2020**, *20*, 526-533.
- [10] Y. Wang, W. Gao, X. Shi, J. Ding, W. Liu, H. He, K. Wang, F. Shao, *Nature* **2017**, *547*, 99-103.
- [11] a) R. Karki, T. D. Kanneganti, *Nat. Rev. Cancer.* **2019**, *19*, 197-214; b) Y. Shi, T. Lammers, *Acc. Chem. Res.* **2019**, *52*, 1543-1554; c) D. A. Erkes, W. Cai, I. M. Sanchez, T. J. Purwin, C. Rogers, C. O. Field, A. C. Berger, E. J. Hartsough, U. Rodeck, E. S. Alnemri, A. E. Aplin, *Cancer Discov.* **2020**, *10*, 254-269; d) Z. Zhang, Y. Zhang, S. Xia, Q. Kong, S. Li, X. Liu, C. Junqueira, K. F. Meza-Sosa, T. M. Y. Mok, J. Ansara, S. Sengupta, Y. Yao, H. Wu, J. Lieberman, *Nature* **2020**, *579*, 415-420; e) Q. Wang, Y. Wang, J. Ding, C. Wang, X. Zhou, W. Gao, H. Huang, F. Shao, Z. Liu, *Nature* **2020**, *579*, 421-426.

**Entry for the Table of Contents**

A general platform to engineer vesicular nanodevices with tunable permeability based on responsive polyion complex vesicles was provided. The formulated GOD-loaded therapeutic nanoreactor with self-boosting catalytic glucose oxidation due to membrane permeability enhancement during ROS production could achieve cytotoxic function via pyroptosis-mediated immunogenic cell death followed by glucose starvation (i) and oxidative stress induction (ii).